Journal of Hydrology: Regional Studies 50 (2023) 101571

Contents lists available at ScienceDirect

Journal of Hydrology: Regional Studies

journal homepage: www.elsevier.com/locate/ejrh

Four decades of lake surface temperature in the Northwest Territories, Canada, using a lake-specific satellite-derived dataset

Gifty Attiah [a,*], Homa Kheyrollah Pour [a], K. Andrea Scott [b]

[a] Remote Sensing of Environmental Change (ReSEC) Research Group, Department of Geography and Environmental Studies, Wilfrid Laurier University, 75 University Ave, West, N2L 3C5, Canada
[b] Department of Systems Design Engineering, University of Waterloo, 200 University Ave, West, N2L 3G1, Canada

ARTICLE INFO

Keywords:
Lake surface temperature
Landsat
Northwest Territories (NWT)
Lake Ice
Climate change
Sub-Arctic
Remote sensing

ABSTRACT

Study region: This study analyzed lake surface temperature (LST) trends and spatial distribution across 535 predominantly small to medium lakes across the North Slave Region (NSR) of the Northwest Territories (NWT), Canada.
Study focus: The NWT is characterized by a vast number of lakes covering a significant portion of its spatial extent. However, there is limited knowledge of how LST responds to climate warming in this region. To address this, LST was analyzed in four distinct periods: open water season (OW), ice cover season (IC), and the transitional months of May (T_M) and October (T_O). LSTs from 1984 to 2021 were retrieved from a lake-specific satellite-derived LST dataset (North Slave LST). LST trend distribution and relationships were analyzed using the Mann-Kendall test and a multilinear regression model.
New hydrological insights: The analysis revealed an overall increase in LST, with average rates (max) of 0.03 °C/year (0.05 °C/year), 0.03 °C/year (0.06 °C/year), and 0.13 °C/year (0.27 °C/year) for OW, T_M, and T_O, respectively accross study lakes. A faster rate of change was observed in October compared to other periods. Results indicated significant increases in LST for 411 lakes (77%) during OW, 418 lakes (78%) during T_O, and 490 lakes (92%) during T_M. The spatial distribution and magnitude of LST change were primarily influenced by geographical than morphometric properties. The analysis demonstrated later freeze-up (0.20 day/year) and earlier break-up (−0.17 day/year) of lake ice across the NSR.

1. Introduction

High-latitude regions, including Canada's north, are experiencing increased air temperatures across their landscapes (Carpino et al., 2018; Eichler et al., 2013; Laing and Binyamin, 2013; Sharma et al., 2019). Lakes comprise a significant part of this landscape, and the processes they undergo - some of which are indicated by the lake temperature - are reacting to these shifting air temperatures. Lakes are crucial in local energy and water cycles and are vital to surface-atmosphere interactions. The vulnerability of these interactions and other Arctic/sub-Arctic systems to climate change has been recognized by various studies (Dauginis and Brown, 2021; Huang et al., 2017; Lang et al., 2021).

Lake temperature drives several hydrological and ecological processes, including turnover, evaporation, energy flow, nutrient

* Corresponding author.
E-mail address: gattiah@wlu.ca (G. Attiah).

https://doi.org/10.1016/j.ejrh.2023.101571
Received 8 June 2023; Received in revised form 9 November 2023; Accepted 11 November 2023
Available online 18 November 2023

cycling, photosynthesis, respiration, and rates of growth and development (De Stasio et al., 2014; Sima et al., 2013), and serves as a significant proxy for regional climate and weather variability (Schneider and Hook, 2010). Critical processes affecting lake conditions, such as ice formation/decay and lake productivity, are impacted by the diurnal and seasonal temperature cycles of the lake (Lang et al., 2021; Reinart and Reinhold, 2008). Furthermore, lake temperature is an essential variable in the development of models for monitoring lake processes, including heat and mass exchanges (Bengtsson, 2012; Echeverría et al., 2019), lake ice phenology (Leppäranta and Wang, 2008; Yang et al., 2012) and lake productivity (Hillmer et al., 2008; Peterson et al., 2016). While evidence has been presented regarding the warming of large lakes on a global scale (O'Reilly et al., 2015), monitoring lakes on a local scale, particularly medium/small size lakes, has received less attention. Lake studies at a local scale can provide a closer look at the impact of region-specific environmental and climate changes on the thermal structure of lakes, which can be transferable to other lakes with similar local conditions.

Satellite remote sensing is a robust tool for providing long-term temporal and spatial data for monitoring freshwater resources, including lakes. Consequently, freshwater surface temperature datasets have been generated from satellite sensors like MODIS (Moderate Resolution Imaging Spectroradiometer) and AVHRR (Advanced Very High-Resolution Radiometer) to enable continuous monitoring of lake surface temperature (LST) (Carrea and Merchant, 2019; Guo et al., 2022; Lieberherr and Wunderle, 2018; Qin et al., 2022). However, the moderate spatial resolution (~1 km) of these sensors' data limits their application to medium/small lakes. On the other hand, data derived from Landsat, with its relatively higher spatial resolution (30–120 m), has proven effective in monitoring several ecological and physical processes in small lakes (Huang et al., 2017; Ogilvie et al., 2018; Prats et al., 2018). Moreover, the availability of thermal bands in Landsat-5 TM, Landsat-7 ETM+ , and Landsat-8 OLI/TIRS allows for the retrieval of the Earth's surface temperature using various algorithms (Avdan and Jovanovska, 2016; Hook et al., 2004; Jiménez-Munoz and Sobrino, 2003; Sobrino et al., 2004; Vanhellemont, 2020). Therefore, the North Slave LST dataset derived from the Landsat satellite series (Attiah et al., 2023) provides a suitable medium through which surface temperature trends and distribution on medium/small lakes can be actively

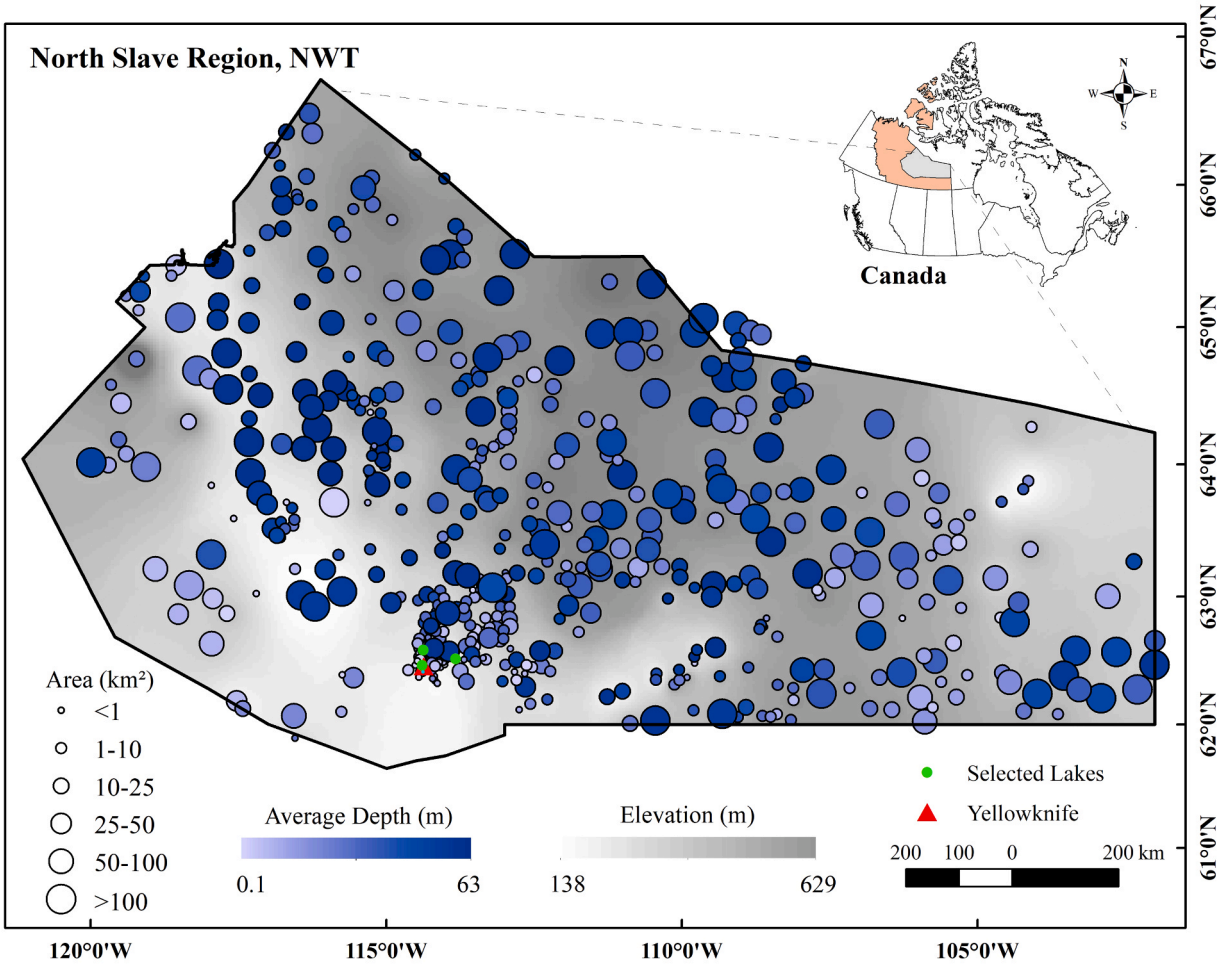

Fig. 1. Geographic distribution of study lakes in the North Slave Region in southeast Northwest Territories, Canada. The circle size denotes the lake area, while the varying shades of blue highlight the difference in lake depths, and the increasing shades of grey show the elevation of the entire region.

monitored.

In the Northwest Territories (NWT), temperature trends and seasonal cycles have been studied in large lakes, such as the Great Slave Lake and Great Bear Lake (Long et al., 2007; Kheyrollah Pour et al., 2012); however, this has not been extended to several medium/small lakes in this region. Unlike large lakes, where heating is greatly influenced by thermal mixing, the cooling and heating of medium/small lakes are governed primarily by overlying air masses (Petrone et al., 2000; Rouse et al., 2005). Therefore, temperature trends on large lakes may not be generalized to medium/small lakes. With over 10,000 medium/small lakes (<100 km^2) in the NWT and a prevalence of lakes smaller than 10 km^2, these water bodies play a substantial role in surface evaporation and the release of sensible heat into the atmosphere (Rouse et al., 2005). In addition, these lakes incorporate several factors related to the regional role of lakes in the surrounding climate, including changes in water levels, evaporation, ice freeze-up, and break-up processes, and stream runoff (Flato and Brown, 1997; Ménard et al., 2002; Rouse et al., 2008). Consequently, it is essential to investigate how these lakes respond to the changing climate, and monitoring LST is one approach to achieve this.

This study examines the long-term temporal and spatial trends in LST of predominantly medium/small lakes in the North Slave Region (NSR), NWT using LST data obtained from the North Slave LST dataset (Attiah et al., 2022). The spatial distribution and time series analysis of LST from 1984 to 2021 (38 years) were conducted for 535 lakes. Lake surface warming or cooling is influenced by several factors, including solar radiation, ice cover duration, the timing of winter lake inverse stratification, spring stratification onset, and air temperature (Mason et al., 2016; Van Cleave et al., 2014; Ye et al., 2019). These processes occur over cold, warm, and transitional periods between the two seasons. However, many studies focusing on LST trends have primarily examined only the ice-free season (Bachmann et al., 2019; Crosman and Horel, 2009; Huang et al., 2017; Lieberherr and Wunderle, 2018; Xie et al., 2022).

This study aimed to analyze the trends and distribution of LST throughout the year, focusing on four distinct periods. These periods include the open water season (OW), ice cover season (IC), and transitional months May (T_M) during the lake ice break-up process and October (T_O) during the freeze-up process. Monitoring ice surface temperature is essential as it includes not only the temperature of the ice surface but also snow and melt-ponds, providing valuable insights into energy balance at the ice surface, driven by the energy exchange between the ice layer and the atmosphere. Additionally, studying the transitional months allows us to understand changes occurring during the freeze-up and break-up periods, which are particularly sensitive to climate change. Furthermore, additional analysis was conducted to gain a comprehensive understanding of LST changes in this region while examining the relationship between LST and various lake properties and external factors, including location, volume, elevation, annual variation, water body surface area, and depth.

2. Methodology

2.1. Study area and lakes

This study examined lakes with varying sizes and depths across the NSR, which lies between latitudes 61°N and 67°N and longitudes 120°W and 102°W of the NWT, Canada. The approximate area of the region is 316,000 km^2 with an average elevation of 301 m, and annual mean air temperature ranges from ~ -45 °C to $+30$ °C. The study region is in the Slave province of the Canadian Shield and is considered a lake-rich region, interspersed with numerous lakes (>10,000). NSR is the most populated administrative region in NWT and home to the capital and largest community in NWT, Yellowknife.

Trends and distribution were studied for 535 lakes (Fig. 1) in the NSR. These lakes were selected because they are widely distributed across the NSR with varying depths and sizes, classified as lakes and not ponds, allowing for obtaining sufficient LST values within the lake boundary. Furthermore, they serve as essential transportation routes during winter, with ice roads constructed across them to facilitate the movement of people, goods, and services. This practical utility underscores their significance in the local and regional context. Additionally, the existing surface temperature data for these lakes allows for studying the dynamics of lake temperatures, especially in the context of climate change, which offers insights into various related processes, including assessments of water quality, the health, and distribution of aquatic ecosystems, as well as adequate water resource management and conservation.

The elevation of lakes ranged from 138 m to 629 m (Messager et al., 2016), while the spatial area ranged from 0.05 km^2 to 1680 km^2 with a known average depth between 1 m and 63 m, as well as volume from 0.24 km^3 to 27321 km^3. Lakes in this region play diverse roles in the surrounding communities and environment, including providing drinking water, fishing, transportation, wastewater reception, and irrigation. In addition, they have individual unique properties with different hydrological regimes of rivers discharging into some of them.

2.2. Data

2.2.1. North Slave LST dataset

Available LST data for all study lakes was obtained from the open-access North Slave LST dataset (https://doi.org/10.5683/SP3/J4GMC2) (Attiah et al., 2022). This dataset provides gridded information on lake surface temperature on a 30-meter grid for 535 lakes in the NSR of the NWT. The dataset covers the period from 1984 to 2021 and was generated by applying a single channel (SC) retrieval algorithm to the thermal bands of Landsat archives (Landsat-8 OLI/TIRS (Operational Land Imager and the Thermal Infrared Sensor), Landsat-7 ETM+ (Enhanced Thematic Mapper Plus), and Landsat-5 TM (Thematic Mapper)). The SC method relies on approximating the radiative transfer equation, eliminating the need for dependence on in situ radio-sounding data. The retrieval process included transforming digital numbers to spectral radiance using metadata information for Landsat images, deriving brightness temperature from radiance values, performing atmospheric and emissivity corrections, cloud masking, specific lake surface temperature

extractions, and data and quality assessment (Attiah et al., 2023). The accuracy of the North Slave LST dataset was assessed in a validation study using in situ and other satellite observations (MODIS) by Attiah et al. (2023), which reported good agreement with the root mean squared deviation (RMSD) of 1.71 °C.

The North Slave LST provides spatially distributed LST data throughout the year with varying temporal resolutions depending on the availability of input data and cloud cover distortions. As a result, the dataset offers more extensive coverage during the OW (57.3%) compared to the IC. LST values were derived for a given day on lakes when at least 10% of the lake's total spatial area was captured. Additionally, each lake had a minimum of 20 images per year, allowing for assessment of the spatial distribution of LST across the region for a given day, as well as time series for individual lakes. Finally, a 100-meter inward buffer was applied to each lake in the dataset to minimize the influence of land pixels on LST due to sensor footprint overlap with the land/lake boundary. For further details about the dataset and retrieval algorithm, refer to the data description provided by Attiah et al. (2023).

2.2.2. Ancillary data

Lake depths and sizes used in this study were primarily obtained from the HydroLAKES database. HydroLAKES is a collation of databases and a digital map repository that includes lakes with a surface area greater than 10 ha (0.1 km^2) and comprises shoreline vector polygons of over 1427,688 individual lakes (Messager et al., 2016). The HydroLAKES database incorporates global and regional databases such as the CanVec series (Natural Resources Canada, 2013) and the SRTM Water Body Data (SWBD; Slater et al., 2006). Average lake volumes and depths for lakes were derived using a geo-statistical model based on surrounding land surface topography. The elevation data in HydroLAKES is calculated using the mode of pixel-level lake elevation data from the Earth-Env-DEM90 digital elevation model and the GTOPO30 DEM provided by the United States Geological Survey (Messager et al., 2016). To assess the spatial evaluation of the North Slave LST dataset, a comparison was conducted using the MODIS (MYD11_L2) surface temperature dataset from 2003 to 2021. Daytime measurements on a ~1 km spatial resolution were compared against the North Slave LST.

2.3. Data analysis

2.3.1. LST trends and distribution

Trends and distribution in LST were categorized and analyzed for four distinct periods: (i) ice cover season (IC) (November to April); (ii) open water season (OW) (June to September); (iii) transitional months May (T_M) and (iv) transitional months October (T_O). IC is the period when lakes are covered with ice and mean LST is less than 0 °C, OW is when lakes are vastly ice-free and mean LST is greater than 0 °C, T_M is the transition period from IC to OW, and T_O is from OW to IC. These periods were chosen because it best captures the LST behaviour of most medium/small lakes in the NSR region. Investigating LST trends and variabilities during different seasons is crucial for understanding annual lake processes and provides further insight into changes occurring on seasonally ice-covered lakes.

To conduct the analysis, individual lake zip files and tab files with lake properties were acquired from the North Slave dataset. The distribution of North Slave LST observations for the four periods studied was 37% for the IC, 13.9% for T_M, 43.4% for OW, and 5.3% for T_O. Further processing was performed, including the extraction of LST times series from gridded data, to enable the application of data analysis techniques. Daily mean, median, maximum, and minimum LST values for all lakes during OW, IC, T_M, and T_O were computed for the analysis. Lake attributes were connected to their respective lakes based on the properties file in the North Slave LST dataset. Additionally, the raw gridded data was used for spatial intra-lake analysis.

The Mann-Kendall test was applied to analyze the long-term distribution trends in LST from 1984 to 2021. This test is robust in detecting statistically significant trends in long-term data (Kendall, 1975). This test's null hypothesis (Ho) suggests no trend, meaning the observations were randomly ordered in time, while the alternative (H_a) represents an increasing or decreasing trend. The Mann-Kendall test is particularly suitable for non-Gaussian distributed data or time series with noisy or missing observations and hence adjudged as a standard method for trend testing (Sen, 1968). Parameters such as the S statistics, Z statistics, and Kendall's tau were considered in identifying decreasing or increasing trends in LST. For trend analysis on individual lakes, a non-parametric test was chosen over the parametric test due to the unevenly distributed and missing data among the lakes, a characteristic of our input time series.

Yearly anomalies were calculated to examine the annual deviation from the mean over the study period and the nature of trends to determine colder and warmer years. The intra-annual transition of overall mean LST was highlighted using the moving-average technique, which calculates a succession of averages across time series data. A 15-day moving average was applied to the interannual mean LST plot for all study lakes for a given day to smoothen the LST to a point where the differences between 1995 and 2021 are highlighted clearly (Kuchar et al., 2019). LST spatial variability and deviations were evaluated based on computations from the standard deviation (SD) to detect the extent of variability in a given dataset. Higher values in SD indicate a more significant variability across the study and vice versa. Trend significance was assessed at $p < 0.05$ unless otherwise stated.

2.3.2. Deviations and relationships between datasets

To evaluate deviations and relationships between the North Slave LST dataset and other datasets, the RMSD, mean bias deviation (MBD), and R-squared were applied. The RMSD quantifies the total divergence between two datasets without distinguishing between over- or under-prediction. A value of 0 for the RMSD indicates no deviation between the values compared. The MBD assesses both the under-prediction and over-prediction between two datasets and identifies systematic differences. The R-squared (R^2) assesses the extent to which independent variables can explain a variation of a dependent variable. In this study, it was used to describe the dependency of LST trends on lake variables across various morphological and geographical gradients. Pearson's correlation (R) was used

to measure the statistical relationship, or association, between LST and other variables.

3. Results

3.1. Spatial distribution of lake surface temperature

3.1.1. Spatial comparison of North Slave LST to MODIS LST

To evaluate the deviation of long-term LST used in our analysis from other LST datasets, a comparison was made between the North Slave LST dataset, and the lake surface temperature obtained from MODIS. This comparison focused on study lakes larger than 5 km^2, totalling 314 lakes, from 2003 to 2021. For each lake, RMSD was calculated to assess the differences between the North Slave LST dataset and MODIS LST. The calculated RMSD values ranged from 2 °C to 5 °C, as shown in Fig. 2a. Across the lakes in the North Slave region (NSR), those with smaller surface areas generally exhibited higher RMSD values (Fig. 2b). The higher RMSD values observed in lakes with smaller surface areas can be attributed to the relatively lower spatial resolution of MODIS LST pixels over such lakes. This lower resolution may result in mixed pixels that include land or small islands within the lakes, resulting in higher RMSD values when compared to pure water pixels of North Slave LST datasets. North Slave LST dataset proved comparable with MODIS; however, the LST deviation between the datasets was more prominent with decreasing lake surface area.

3.1.2. Spatial variation of mean LST

The spatial variation of mean LST across lakes in the study region from 1984 to 2021 was investigated. Mean LST values ranged from − 7.6 °C to 5.1 °C (Fig. 3). LST ranges across the region for the four time periods (OW, IC, T_M, and T_O) ranged from 5 °C to 19.5 °C (OW), − 22.9 °C to − 14.7 °C (IC), − 6.4 °C to 8.1 °C (T_M) and − 10 °C to 3 °C (T_O). Among these periods, IC had the lowest variation in LST (SD = 1.9 °C), while T_O showed the highest variation (SD = 3 °C). Lakes located further east in the region recorded the coldest LSTs, whereas those in the southwest were relatively warmer. The warmest lakes, however, were within and surrounding the city of Yellowknife, the largest urbanized area in that region. Relatively high temperatures were observed in smaller lakes (< 1 km^2), such as Joe Lake (0.1 km^2) (62.483, −114.387), Pud Lake (0.2 km^2)(62.432, −114.385), and Meg Lake (0.1 km^2) (62.416, −114.383), within the Yellowknife area. Lakes at higher elevations (> 400 m) generally recorded lower mean LST. Fig. 3b and Fig. 3c show the distribution of mean LST across all the study lakes' sizes and depths, respectively, which showed that generally, mean LST in larger and deeper lakes were lower and had a smaller range.

As shown in Fig. 3, the spatial distribution of LST was influenced by location, lake size, depth, and elevation. A multivariate regression analysis was conducted to understand further the importance of topography, morphometry, and geographical location to the spatial distribution of LST in the NSR. Five independent variables retrieved from the HydroLAKES database were used in the analysis. The possible explanatory factors explored included lake size and depth for the morphometric characteristics, elevation for the topography, and longitude/latitude for geographical location. This method has proven efficient in previous applied and theoretical studies (Magee and Wu, 2017; Woolway et al., 2017). Mean LSTs for all 535 lakes for each period were regressed on the five predictor variables to understand the distribution of LST in the region. All variables were normalized to a range from 0 to 1 to set a standard scale

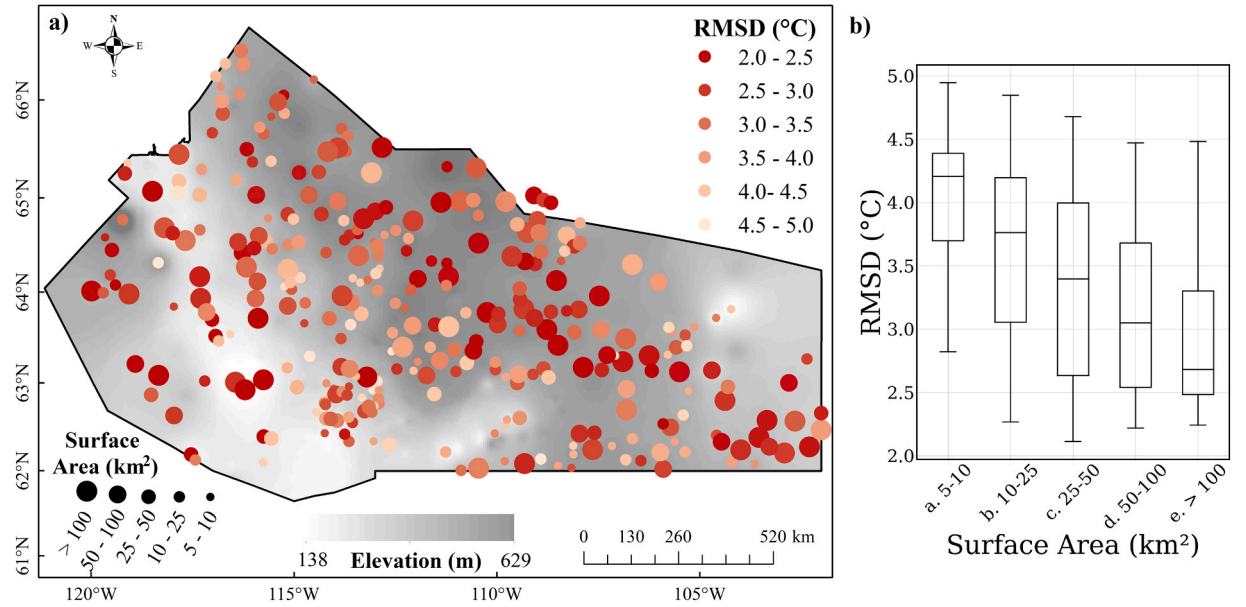

Fig. 2. a) RMSD distribution of North Slave LST evaluated against MODIS LST (2003 – 2021) for lakes (314) in study area b) boxplot of RMSD distribution related to lake surface area.

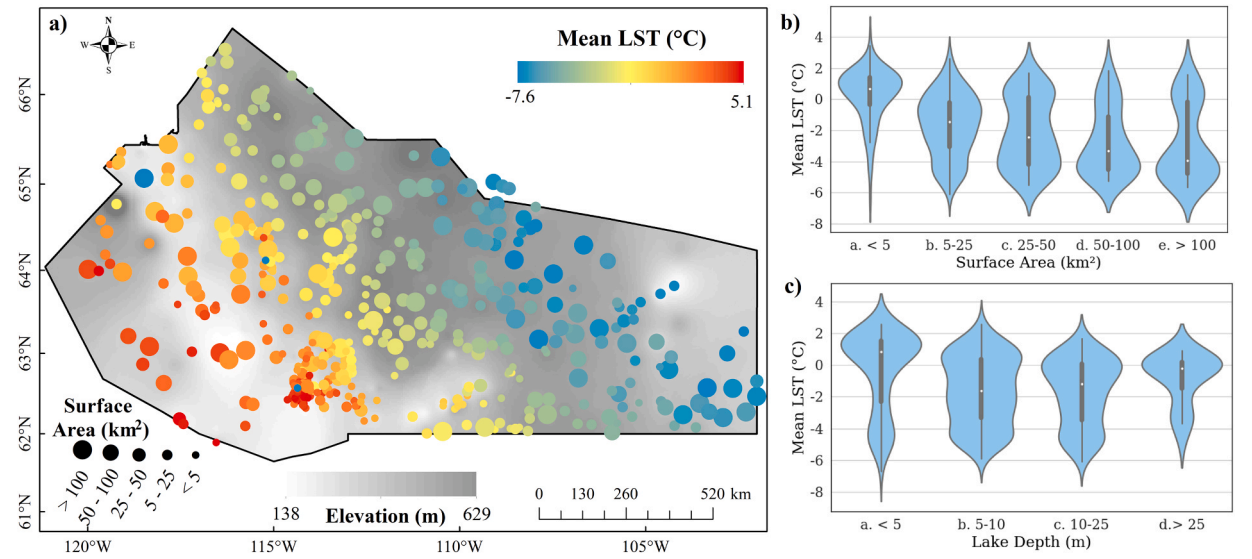

Fig. 3. Spatial distribution of mean lake surface temperature from 1984 to 2021 in the North Slave region and its relations to b) surface area of lakes and c) lake depth.

due to their different measurement units. The regression model results are summarised in Table 1.

The model indicated that the combined predictor variables accounted for a substantial portion of the variance (R^2) in mean LST: 92% for IC, 86% for OW, 87% for T_M, and 68% for T_O. Mean LST showed a positive relationship with lake depth for IC (1.3) and T_O (5.3). Elevation had strong relationships with mean LST for all periods, ranging from − 0.8 to − 4.0. Elevation explained up to 20% of the variance (R^2) in mean LST in OW. Longitude and latitude had strong negative relationships for all periods, ranging from − 4.3 to − 10.3, with the strongest in T_O (−8.6) for latitude and T_M for longitude (−10.3). Longitude explained 87%, 69%, and 68% of the variance in LST for the IC, T_M, and OW, respectively; however, it explained only 29% for T_O, as indicated by the partial R^2 values.

3.2. *Temporal distribution of lake surface temperature*

Fig. 4 illustrates the seasonal variations in the LST distribution for the 535 lakes studied in the NSR region. The analysis is based on

Table 1
Multivariate Linear regression model summary for predicting mean LST for each during ice cover season (IC), open water season (OW), transitional months - May (T_M), and October (T_O).

Dependent Variable	Independent Variable	Coefficient	Standard Error	Partial P-Value	Model P- Value	VIF	Partial R^2	R^2
Mean LST (IC)	Intercept	-12.982	0.080	< 0.001	< 0.001		0.980	0.923
	Depth	1.308	0.215	< 0.001		1.224	0.067	
	Size	-0.476	0.296	0.109		1.093	0.005	
	Elevation	-0.808	0.183	< 0.001		1.808	0.036	
	Longitude	-8.733	0.144	< 0.001		1.624	0.877	
	Latitude	-4.363	0.144	< 0.001		1.967	0.639	
Mean LST (T_M)	Intercept	8.187	0.171	< 0.001	< 0.001		0.817	0.860
	Depth	-3.386	0.457	< 0.001		1.224	0.097	
	Size	-2.318	0.630	< 0.001		1.093	0.026	
	Elevation	-4.045	0.390	< 0.001		1.808	0.173	
	Longitude	-10.333	0.306	< 0.001		1.624	0.689	
	Latitude	-7.077	0.307	< 0.001		1.967	0.508	
Mean LST (OW)	Intercept	20.600	0.151	< 0.001	< 0.001		0.973	0.872
	Depth	-3.991	0.403	< 0.001		1.224	0.160	
	Size	-4.943	0.556	< 0.001		1.093	0.133	
	Elevation	-3.908	0.344	< 0.001		1.808	0.200	
	Longitude	-8.705	0.270	< 0.001		1.624	0.668	
	Latitude	-6.654	0.272	< 0.001		1.967	0.539	
Mean LST (T_O)	Intercept	2.830	0.255	< 0.001	< 0.001		0.194	0.682
	Depth	5.328	0.680	< 0.001		1.224	0.107	
	Size	-1.286	0.938	0.171		1.093	0.004	
	Elevation	-3.954	0.581	< 0.001		1.808	0.083	
	Longitude	-6.604	0.456	< 0.001		1.624	0.289	
	Latitude	-8.581	0.458	< 0.001		1.967	0.406	

the combined mean LST from 1984 to 2021, with a specific focus on the years 1985 (the first year with a complete record from January to December) and 2021 (the last year of the study period). From November to April, lakes in this region typically experience negative temperatures, with the lowest temperatures occurring in early January (Day of Year (DOY) = 13). During the IC, the presence of ice and snow on the lake surface insulates the water from the atmosphere, causing satellite-derived LST to be more indicative of air temperature and surface radiation than during the OW. Variations in LST values may occur due to the presence of snow or melt ponds on the surface.

The majority of lakes in this study experience a transition from ice-covered to open-water seasons, and vice versa, in May and October, respectively, which are considered transitional months. During this period, LST is derived from a combination of ice and water pixels. October is the month when LST decreases to 4 °C (DOY = 265), corresponding to the temperature at which freshwater reaches its maximum density. When this temperature is reached, turnover occurs in the water column, resulting in colder surface water than at the lake bottom (Bengtsson, 2012). The average LST further decreases to 0 °C in early October (DOY = 280), indicating the initial formation of ice and the beginning of the ice-covered season. In contrast, May is characterized by an increase in surface temperature from the ice-covered season, with the temperature reaching around 0 °C in mid-May (DOY = 138) and rising above 4 °C in the last week of May (DOY = 149). This period is characterized by rising air temperatures, increases in solar radiation, diminishing ice cover, and albedo, all contributing to the increase in surface temperature.

Mean LST during OW demonstrated a monotonically positive increase from June to early August, reaching the highest temperature in early August (DOY = 214) and subsequently declining throughout September. September temperatures varied among lakes and across years, primarily influenced by the maximum air temperatures during summer (Reinart and Reinhold, 2008). In general, LST values demonstrated variations throughout the year, with a consistent peak in late July or early August observed for multiple years.

Differences were observed across the four time periods when comparing the inter-annual changes in LST between two years (1985 and 2021). The minimum mean LST during the IC period for 1985 was − 35.3 °C, while in 2021, it was − 26.7 °C. The OW showed generally lower mean LST values in 1985 compared to 2021. During the transitional month of October, LST dropped below 0 °C earlier in 1985 (DOY = 280) than in 2021 (DOY = 284). Negative temperatures persisted in 1985, reaching 0 °C later (DOY = 168) compared to 2021 (DOY = 124). LST for 1985 was lower (−12.8 °C) compared to the overall mean (−1.7 °C), whereas for 2021, it was relatively high (−4.0 °C) across the entire year.

The distribution of LST for each year was analyzed for all 535 lakes in the study. Ridgeline charts were used to illustrate changes in LST from 1984 to 2021, representing the four time periods (Fig. 5). The results showed a notable LST shift towards higher temperatures for OW, T_M, and T_O from 1984. Particularly, T_O showed more substantial shifts towards higher LSTs than OW, IC, and T_M. IC had more variability from 1987 to 2000, 2005–2014, and 2015–2021. T_M was characterized by the majority of lakes with LST values close to 0 °C, with more lakes having negative LST values than positive in earlier years (pre-2005). OW also shifted towards higher LST, with a left-skewed distribution that intensified over time. T_O showed diverse LST distribution patterns across the years, featuring bi-modal distributions towards colder LST in earlier years and a shift towards warmer LST in later years (post-2004–2005). These results provide insights into the general trends of LST, indicating that LST variability and shifts over time are not similar across the four time periods, albeit generally shifting towards warmer temperatures.

3.3. Seasonal trends and interannual variability of LST

The variations in annual LST were further investigated using yearly anomalies for the four time periods, calculated based on the average LST for the study period (1984 – 2021) as the reference. Anomalies observed in IC fluctuate over the years as expected, with temperature anomalies for IC generally between − 5 °C and 7 °C (Fig. 6). Among the four time periods, the range of anomalies observed in the OW was the lowest, from − 3.2–2.5 °C. A significant increase was observed in the LST trends recorded for all lakes collectively over the four periods examined in this study using the Mann-Kendall Test. The most pronounced rate of change was

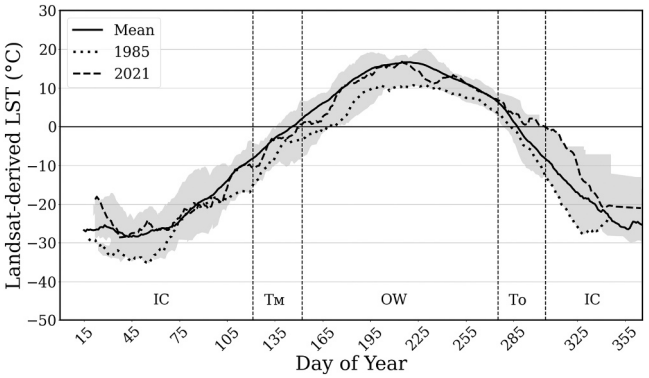

Fig. 4. Average intra-annual variation of mean LST for all lakes (solid line), 1985 (dotted line) and 2021 (dashed line) showing the trend and transitions between periods (ice cover season (IC), open water season (OW), transitional month May (T_M), and transitional month October (T_O)) on a 15-day running mean. Grey areas show the temporal ranges for all individual lakes.

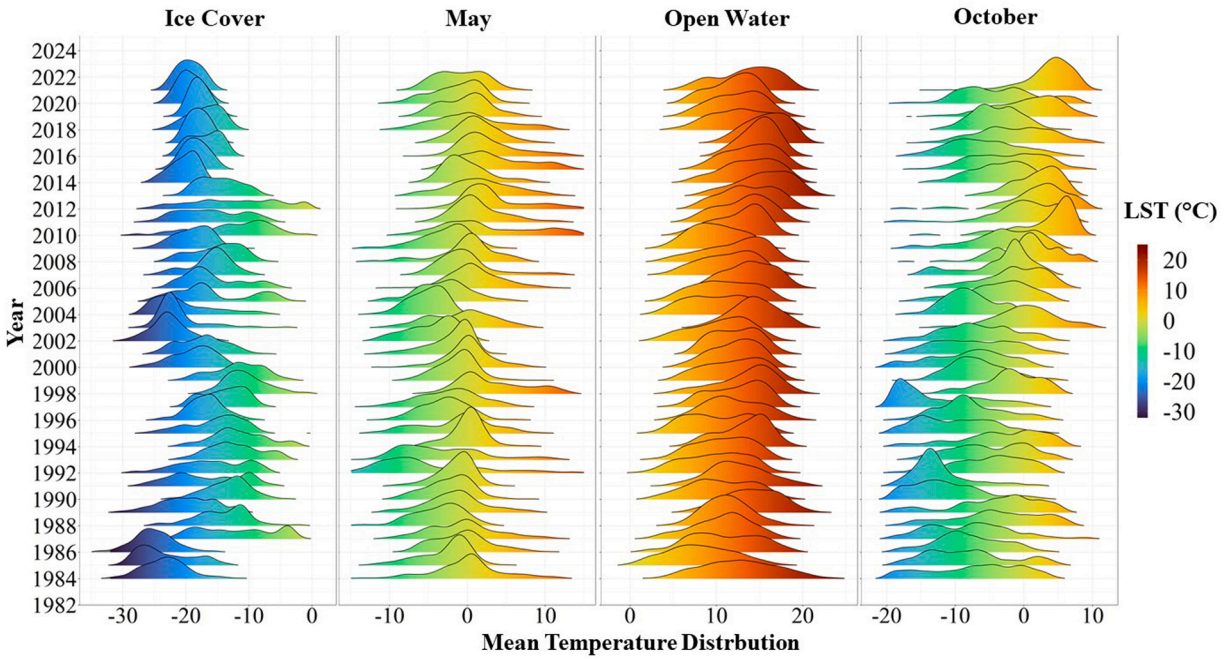

Fig. 5. Yearly distribution LST for 535 lakes from 1984 to 2021 ice cover season (IC), open water season (OW), transitional month May (T_M), and October (T_O).

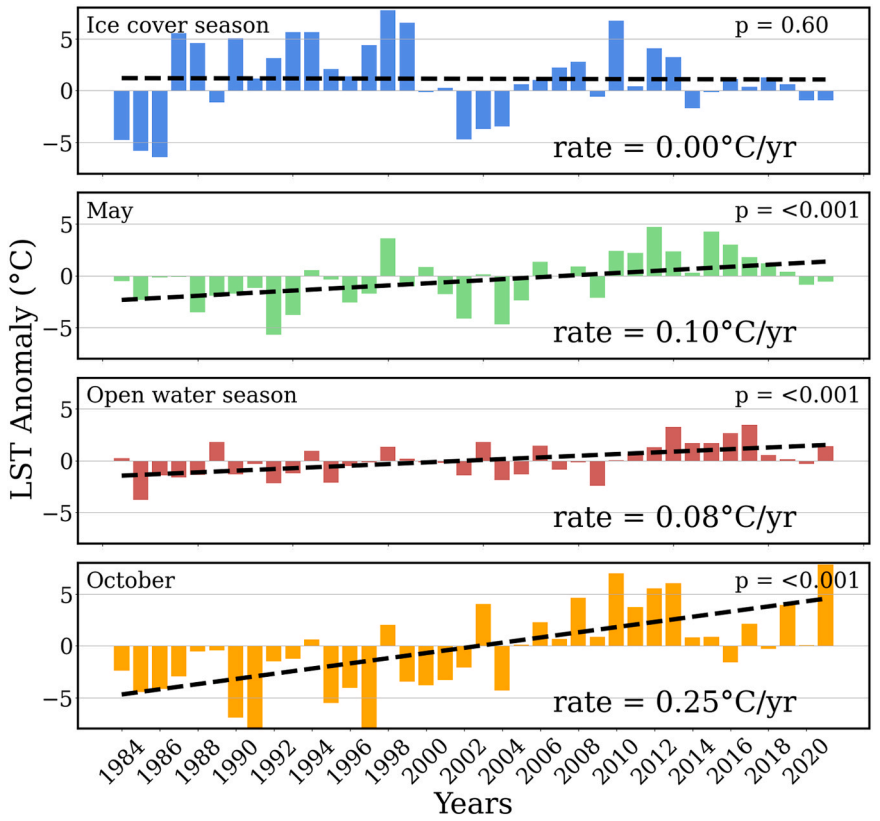

Fig. 6. Lake surface temperature anomalies and trends observed in the ice cover season (IC), transitional months May (T_M) and October (T_O), and open water season (OW) from 1984 to 2021. The black dashed lines represent the trend line.

observed in $T_{O,}$ with the highest anomaly of + 7.8 °C in 2021 for all 535 lakes. In general, T_O showed the highest average rate of change (0.25 °C/year). In contrast, IC showed the lowest average rate of change among all seasons. Trends in the OW (0.08 °C /year), T_M (0.10 °C /year), and T_O were statistically significant ($p < 0.001$), and changes during the IC were not significant at $p = 0.60$.

To further investigate the trend of LST in individual lakes and their spatial distribution, a Mann-Kendall test was applied to determine lakes with statistically significant LST trends from 1984 to 2021 (Fig. 7). Most lakes studied in this region demonstrated an increasing trend in LST. The highest percentage of lakes with a significant increasing trend was in T_M (92%), followed by T_O (78%). However, the highest increase was observed in T_O and mainly centred around Great Slave Lake and Yellowknife. The OW highlighted a greater magnitude of change in higher-elevation areas. In addition, the distribution of significant increases in LST is more widely distributed (spatially) in the OW than in other periods. Trends observed across all individual lakes in IC were statistically insignificant. T_O demonstrated a higher increasing LST trend for individual lakes as well as mean for all lakes (0.13 °C/year) compared to T_M (0.03 °C/year) and OW (0.03 °C/year). On the other hand, OW has the lowest statistically significant LST increase for lakes across the NSR (up to 0.05 °C /year).

Individual lakes across the NSR exhibited variations in the magnitude of LST change. Further analysis was conducted on all study lakes to investigate the factors contributing to this variability. Correlation was calculated between variables (Longitude, Latitude, Volume, Depth, Area, elevation, and distance from Yellowknife) and mean LST (Fig. 8a) and LST rate (Fig. 8b). LST rate showed a negative relationship (−0.14 to −0.45) to variables in the T_M and T_O but a positive relationship (−0.14 to −0.56) in OW and IC. There was generally a negative relationship between Mean LST and the variables. Distance to Yellowknife (−0.74 to 0.81) had the highest correlation to LST.

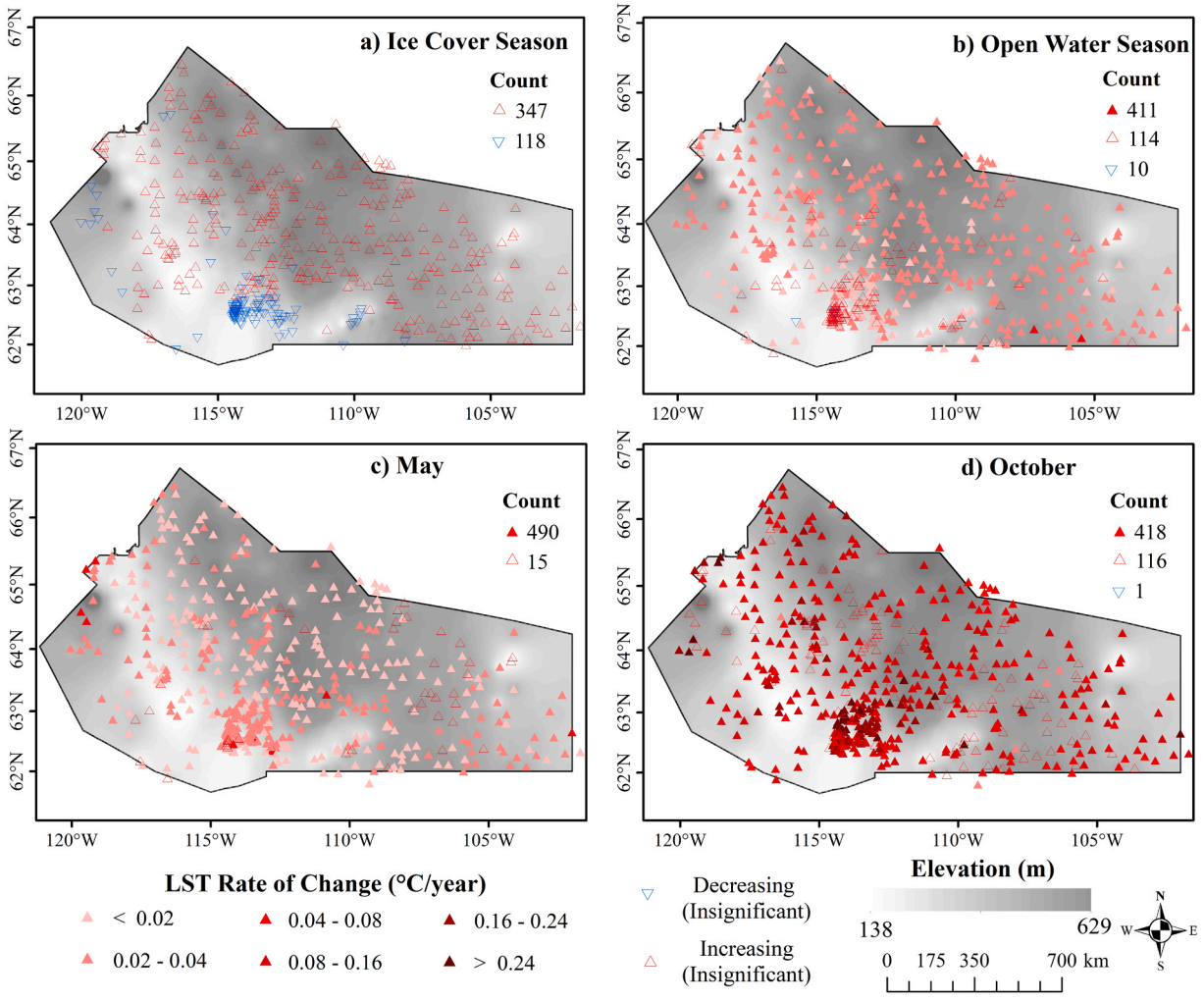

Fig. 7. Significance and distribution of the rate of change observed for all study lakes in the North Slave region from 1984 to 2021 for a) Ice cover season (IC), b) Open water season (OW), c) Transitional month May (T_M), and d) Transitional month October (T_O). Filled triangles indicate statistically significant trends in LST, while hollow ones indicate statistically insignificant trends.

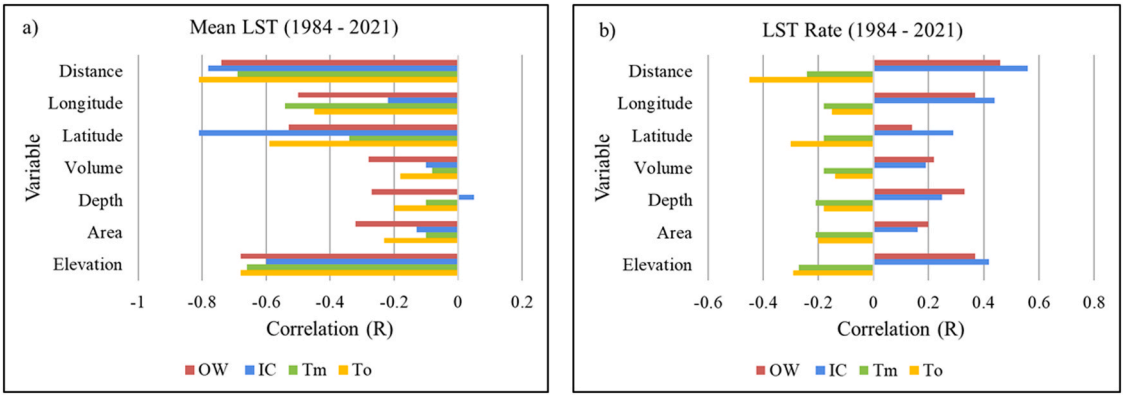

Fig. 8. Correlation between a) mean LST and b) change rate of LST and lake variables for all periods (Distance presents the distance from Yellowknife).

3.4. Intra-lake variation of LST trends on selected lakes

Three lakes near Yellowknife (Jackfish, Small, and Ryan) were selected to better understand their respective patterns of spatial LST change and to observe their trend behavior to comprehend the internal variations in warming within lakes. These lakes were selected based on their relatively comparable atmospheric forcing. At the same time, their differing depths and mixing characteristics offered a unique opportunity to study how these lakes respond to nearly identical climate factors. The lake bathymetry maps, the spatial distribution of LST rate of change within each lake, and the correlation between LST and depth are presented in Fig. 9.

Fig. 9a shows the distribution of the LST rate of change for the three lakes over 38 years (1984–2021). The Mann-Kendall test was applied to each 30 m pixel across the entire lakes during OW. Among the lakes, Ryan Lake exhibited the highest rate of change, with a maximum of 0.17 °C/year, followed by Small Lake (0.14 °C/year) and Jackfish Lake (0.11 °C/year). Fig. 9b shows the depth distribution (bathymetry), with the maximum depth of Jackfish Lake being the shallowest at ~7 m and Small Lake at ~12 m. In contrast, Ryan Lake is the deepest, with a maximum depth of ~90 m. The depths of Jackfish and Small Lakes fall within the typical range for small to medium-sized lakes in the region, unlike Ryan Lake, which is a small and deep subarctic lake with a mean depth of 35.3 m (Rafat et al., 2023). The LST rate of changes across the three lakes shows some variability over the 38-year period, with certain lakes exhibiting higher LST change than others.

Exploring the intra-lake spatial distribution of LST change highlights areas with higher warming rates, which can be further explored to understand the factors contributing to those variations. A positive correlation between the LST rate of change and lake depth was observed using these three lakes as a case study. In Jackfish Lake and Small Lake, deeper parts of the lake appear to have a higher temperature change than shallow parts. However, this behavior was not similarly evident in Ryan Lake. The correlation between depth and LST rate of change for the lakes was found to be the highest for Jackfish Lake at 0.65 ($p < 0.001$), followed by Small Lake at 0.30 ($p < 0.001$) and Ryan Lake at 0.14 ($p = 0.05$) (Fig. 9c). When compared to correlations calculated for a few other lakes (not shown), such as Handle Lake (Depth = 4 m, $R = 0.9$, $p < 0.001$) and Long Lake (Depth = 7 m, $R = 0.5$, $p < 0.001$), a generally positive relationship between intra-lake LST rate of change and depth was observed.

3.5. Lake surface temperature and lake ice phenology

Assessing lake ice phenology provides indications of changing weather and climate conditions. Faster rates of LST warming can be attributed to reduced ice cover during winter. Given that the timing of freeze-up and break-up of lake ice is a good indicator of increasing temperatures and vice versa. This study aimed to investigate how LST reflects freeze-up and break-up dates during the transitional months over the years. LST was used as a proxy to examine lake ice phenology. Previous studies, such as Gou et al. (2017), have reported the LST range recorded for pixels during freeze-up to be between − 1.7 °C and 0 °C, while for break-up, they were between 0.3 °C and 1.7 °C. These ranges influenced the threshold set for freeze-up (when the ice starts to form lakes) and break-up (when ice has melted) adopted in this study. In our study, the end of the break-up period was defined as when the mean LST over the lakes was above 1 °C, and the onset of freeze-up was when it was below − 0.5 °C. Fig. 10 shows the yearly average freeze-up onset and break-up from 1984 to 2021 calculated using mean LST.

Lakes in the NSR are experiencing later freeze-up (0.20 days/year) ($p = 0.09$) and earlier break-up dates (−0.17 days/year) ($p = 0.1$). The collective trend observed in all lakes and the trends demonstrated for individual lakes indicate an increasing rate of warming in lakes within the NSR. The earlier break-up and later freeze-up timings observed throughout the study period underscore the interannual temperature changes occurring in the region. These findings align with several studies that have reported earlier break-up timings and later freeze-up timings for lakes in northern regions (Dauginis and Brown, 2021; Kheyrollah Pour et al., 2017).

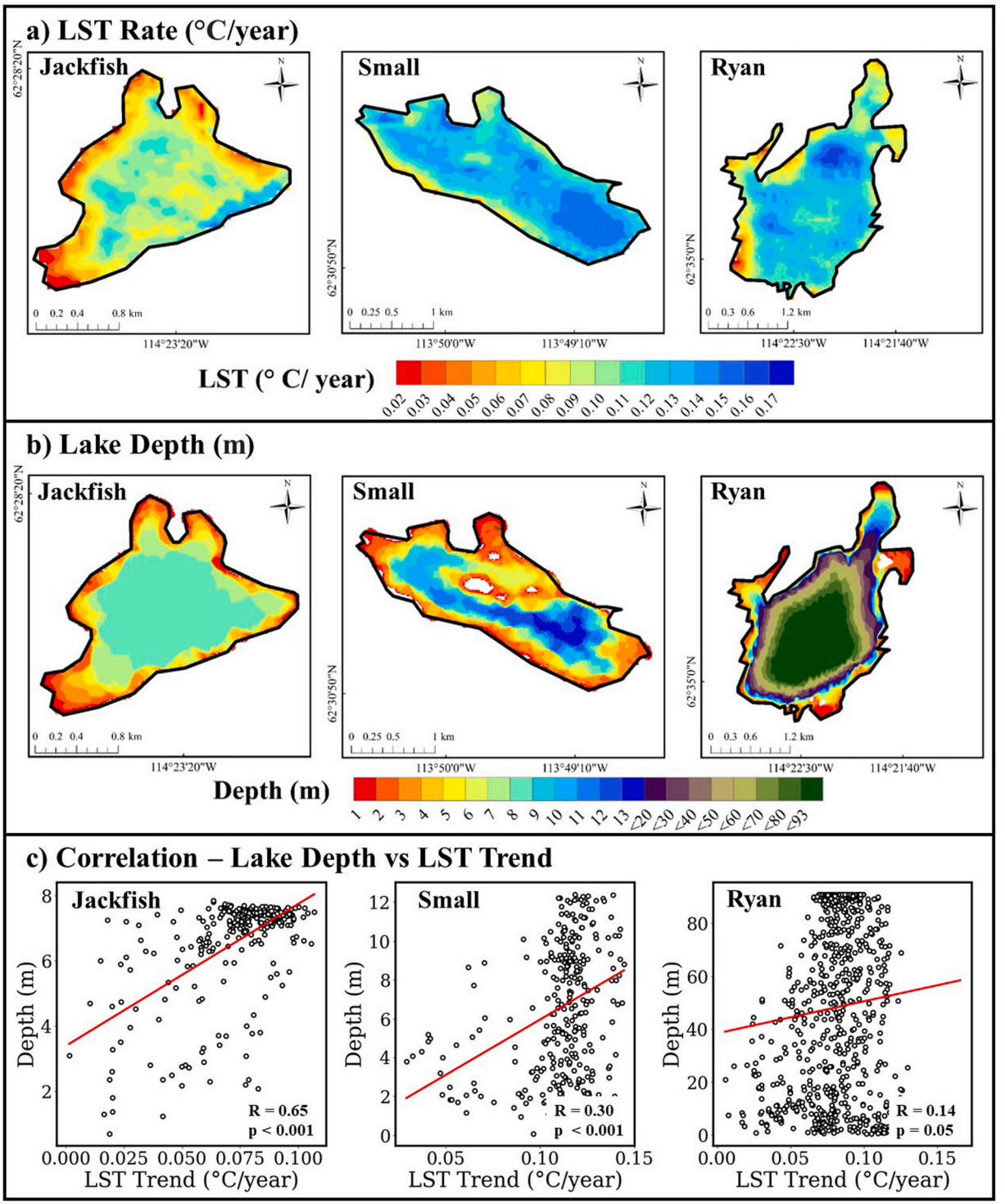

Fig. 9. a) Map shows the distribution of spatial variability of LST rate of change within lakes (Jackfish, Small, and Ryan Lakes) (°C/year), b) Lake bathymetry maps (depth in meters), and c) Correlation (R) between lake depth and LST rate of change.

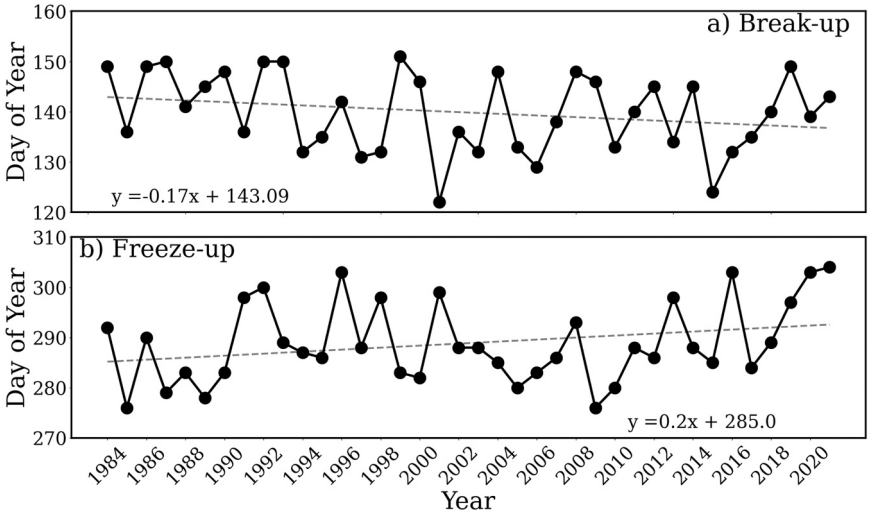

Fig. 10. Trends observed in break-up and freeze-up from 1984 to 2021. Break-up and freeze-up dates were determined from LST thresholds near the freezing point.

4. Discussion

4.1. Lake surface temperature in the North Slave Region

Evaluation of LST trends for 535 lakes in the NSR collectively and individually revealed increased warming rates with time. There was a significant increase in LST for all seasons except the IC for more than 77% of lakes studied from 1984 to 2021, with an average LST increase of 0.03 °C/year observed for OW. These findings corroborate previous studies conducted using different methods, which have consistently demonstrated an increasing trend of LST during OW in various regions worldwide (Dokulil et al., 2021; Song et al., 2016; Stefanidis et al., 2022; Xie et al., 2022; Yang et al., 2020). Notably, October was identified as the month exhibiting the highest rate of change in LST for individual lakes across the NSR and collectively (0.25 °C/year). October, having the highest rate of LST increase, corresponds with a lake study conducted in Austria (Niedrist et al., 2018) that revealed October had the highest (0.88 °C/decade) lake surface warming from 1972 to 2015. This increase was attributed to summer and winter heat storage and absorption of incoming longwave radiation and may be crucial for small seasonally ice-covered lakes (O'Reilly et al., 2015). Generally, ice formation on lakes in the NSR over the years is occurring later, as observed in several other studies of lakes in high-latitude regions (Cai et al., 2019; Tom et al., 2022). We discovered a mean inter-annual delay in ice formation equivalent to 0.20 day/year from 1984 to 2021, resulting in an extended ice-free season, particularly in autumn. A shift towards later ice formation may create positive feedback, where longer heating periods on lakes due to solar radiation absorption (Zhong et al., 2016) can further lengthen the ice-free season.

The variations in LST increases across the NSR are impacted by broad-scale climatic factors such as solar radiation and air temperature (Schmid and Köster, 2016). LST is influenced by heat flux through the water, regulated by longwave radiation, shortwave radiation, and sensible and latent heat fluxes. Solar radiation is reported to be increasing in the Northern Hemisphere (Livingstone, 2003; Matzinger et al., 2007; North et al., 2014), and with decreased cloud cover (Eastman and Warren, 2013), shortwave radiation received at the lake's surface increases (Shinohara et al., 2021). Schmid and Köster (2016) found that solar radiation accounted for 40% of LST increases on European lakes and 60% attributed to air temperature.

Air temperature is reported to be warming at accelerated rates at higher latitudes (IPCC, 2021), with the Earth experiencing a rise of ~1.2 °C since the pre-industrial era (Song et al., 2022). In hydro-ecologically sensitive regions such as the NWT, air temperatures are significantly affected by atmospheric-oceanic circulation patterns like the Arctic dipole (AD) (Persaud et al., 2022). The study by Persaud et al. (2022) conducted in the NWT revealed a predominantly negative AD index between the 1900 s and early 2000 s, as well as between 2002 and 2007, corresponding to the patterns of LST anomalies observed in this study. This convergence suggests a noteworthy correlation between air temperature and LST trends in the NSR. In the future, LST warming rates may be driven higher due to the shorter length of ice cover in the Northern latitudes, which increases the duration of energy absorption, reduces lake albedo, and propels earlier stratification (Austin and Colman, 2007; O'Reilly et al., 2015).

It is essential to recognize that various lake characteristics also modulate the impact of air temperature on LST (Yu et al., 2021). The response of lakes to climate change and LST distribution is found to be influenced by morphometric and geographic properties in addition to climatic factors (O'Reilly et al., 2015; Woolway et al., 2020; Xie et al., 2022). Individual lakes across the NSR exhibited variations in the rate of LST change driven by elevation, longitude/latitude, and distance from Yellowknife. While morphometry substantially influences several lakes, it had minimal impact on the variation observed in the rate of LST change across the NSR.

Lakes closer to Yellowknife had relatively higher surface temperatures than those located further away. Urbanization has been identified as a contributing factor to LST variations (Yang et al., 2020). This study found a strong negative correlation (R= −0.69 to

−0.81) between the distance from Yellowknife and the mean LST for all seasons (Fig. 8a). Additionally, a negative relationship (R = -0.45) was observed between the rate of LST change and the distance between lakes and Yellowknife during the transitional month of October. These findings suggest that lakes' transition from open water to ice cover occurs later near Yellowknife than in more distant regions. Urbanization and its expansion contribute to an increase in impervious surfaces, which absorb heat, thereby impacting the temperature of runoff entering lakes. Additionally, increased human activities can influence regional air convection, land surface temperature, and other factors that contribute to the urban heat budget (Adamowski and Prokoph, 2013), affecting LST. Although the land surface temperature of the NSR has not been explicitly studied previously, the National Centre for Environmental Information (NOAA) reported elevated land surface temperature trends (0.55 °C decade −1 to 0.89 °C decade −1) within the study region (NOAA, 2022).

Geographical properties proved more significant than morphometry in the distribution of LST and rate of change in the NSR. Despite a relatively small range in latitude (61–67°) in our study region (Fig. 1), substantial evidence underscores a robust connection between latitude and LST. Similar conclusions have been drawn in prior studies (Bachmann et al., 2019; Ramón et al., 2020; Woolway et al., 2017). Latitude/longitude accounted for more variance in the distribution of mean LST compared to other variables. Latitude considerably influences the amount of solar radiation received at the surface, with higher latitudes experiencing a smaller angle of incoming solar radiation, resulting in cooler temperatures. Since most lakes in this region are hydrologically isolated (close-basin) lakes, solar radiation is the primary source of heat energy, potentially accounting for the negative relationship observed between mean LST and latitude.

In the present study, the relationship between elevation and the rate of change in LST during OW showed a weak positive correlation (R= 0.37). However, the relationship between elevation and mean LST during the OW was negative and stronger (R = −0.68), indicating that elevation plays a more significant role in explaining temperature variation among lakes than the rate of increase observed in the NSR. We recognize that the highest elevation in our study area is 629 m, making our results region-specific. Differences in maximum elevation and ranges across regions make the relationship between lake elevation and magnitude of LST change very subjective. Existing studies report positive and negative relationships with altitude (Zhang et al., 2019). This elevation and LST change relationship disparities suggest that lake thermal regimes and stratification are influenced by additional external factors, such as snowmelt runoff and cloud cover (Livingstone et al., 2005).

4.2. Dynamics and implication of increasing surface temperature on lakes

In Yellowknife, air temperatures have constantly risen in all seasons over the past 40 years, similar to other sub-Arctic areas, leading to significant impacts on nearby aquatic ecosystems (Sivarajah et al., 2020). The health, behavior, growth, and survival of fish and other aquatic species can be influenced by warmer lake temperatures. Changes in the timing of algal and other planktonic blooms, driven by increasing temperature, can affect fish by altering their food availability and overall ecosystem dynamics (Daufresne et al., 2009). The onset of cyanobacterial blooms, in particular, has been linked to temperatures, and these blooms can lead to reduced dissolved oxygen concentration in the water, creating deoxygenation patterns and posing a threat to aquatic organisms, including fish (Pokhrel et al., 2021; Tye et al., 2022). In addition, higher concentrations of algae and other aquatic vegetation can degrade water quality, posing risks to human health and well-being (Moss, 2012).

The implications of increasing LST and reductions in the ice season length extend to the northern communities surrounding these lakes, particularly in terms of ice road transportation and infrastructure. The Tibbitt to Contwoyto Winter Road (TCWR), one of the world's busiest heavy-haul winter roads, is constructed on some lakes within our study, serving as a vital component of the northern transportation network (Mullan et al., 2017). Warmer temperatures lead to more extended open-water periods, resulting in delayed ice formation and changes in freeze-up and break-up periods of lake ice. These factors significantly impact the timing and construction of ice roads, affecting the natural resource industry and its transportation of goods and resources (Dibike et al., 2011; Mullan et al., 2017). The socioeconomic systems in northern regions, which heavily rely on snow and ice, are particularly vulnerable to continuous warming, as natural resources, infrastructure, and transportation sectors are intertwined with these frozen environments (Pouw et al., 2023; Prowse et al., 2009). Additionally, delayed construction and uncertainty in ice safety limit access to essential resources for communities in the NSR, affecting travel between neighboring communities and alternative supply routes during winter.

5. Conclusion

To the best of our knowledge, this study is the first to examine LST trends on an extensive scale within the Northwest Territories. The study examined the variations of LST over four time periods (IC, OW, T_M, and T_O) from 1984 to 2021 using the North Slave LST dataset derived from Landsat imageries. By investigating LST changes across these periods, the thermal behavior of lakes in the NSR, including the impact on ice phenology, was elucidated, which cannot be fully understood by solely studying the OW. The spatial distribution of LST was influenced by morphometric and geographical factors, accounting for 68–92% of the mean LST variation across the NSR over four periods. An overall warming trend was observed for all seasons from 1984 to 2021 except the ice cover season. Most lakes in the region (77%) experienced significant LST increases during OW, with a mean rate of 0.3 °C/decade, substantiating previous findings. In addition, the annual trends in the transitional months of T_M and T_O were higher than OW, indicating an earlier transition from IC to OW and a later transition from OW to IC. Lakes during the IC demonstrated predominantly insignificant warming trends across the NSR. The magnitude of LST change distribution in the NSR was primarily associated with elevation, latitude/longitude, and proximity to Yellowknife.

Despite this study's best efforts to investigate variables influencing LST, there were some limits and uncertainties. In this study, the

magnitude to which changes in air temperature affect LST remains unexplored due to the unavailability of in situ data, such as air temperature, cloud cover, and incoming radiation on individual lakes, which would enable a more comprehensive analysis. Further research is required for a more comprehensive understanding of the direct impact of LST changes on lake processes, including lake ice freeze-up and break-up processes, algal blooms, and nutrient cycling. Furthermore, continuous research is needed to investigate the relationship between LST changes and other ecological and hydrological systems, thus enhancing our understanding of LST behavior during different periods.

Regional analysis of LST is of utmost importance in comprehending the impact of local environmental and climatic factors and the broader phenomenon of climate change on the trends observed in LST during various periods throughout the year. Acquiring knowledge about the shifting patterns in LST is essential for effectively managing water resources, as it aids in making informed decisions regarding water allocation and conservation initiatives. Moreover, a comprehensive understanding of LST trends can significantly enhance ecological research by offering valuable insights into the influence of LST on the growth, reproduction, and migration patterns of aquatic species such as fish, algae, and other relevant organisms. Furthermore, LST research can inform environmental policies and regulations related to water quality and resource management. Governments and regulatory bodies can use this information to establish guidelines for protecting lakes from temperature-related stressors. Ultimately, continued monitoring of the long-term thermal dynamics of lakes is necessary under the current global warming regime to develop efficient precautionary measures against the impacts of warming and to make informed future projections and decisions.

CRediT authorship contribution statement

Gifty Attiah: Writing – review & editing, Writing – original draft, Visualization, Validation, Methodology, Investigation, Formal analysis, Data curation, Conceptualization. **K. Andrea Scott:** Writing – review & editing, Supervision, Resources, Project administration, Funding acquisition, Conceptualization. **Kheyrollah Pour Homa:** Writing – review & editing, Supervision, Resources, Project administration, Funding acquisition, Conceptualization.

Declaration of Competing Interest

The authors declare that they have no known competing financial interests or personal relationships that could have appeared to influence the work reported in this paper.

Data Availability

The link and citation to the publicly available and published data is included in the manuscript.

Acknowledgement

The authors respectfully acknowledge that this research was conducted within the Chief Drygeese territories on the traditional land of the Yellowknives Dene First Nation. The authors are grateful to the Indigenous Peoples for allowing them the opportunity to learn and conduct fieldwork on their lands. This research has been supported by funding from the Natural Sciences and Engineering Research Council (NSERC) Canada Research Chair (CRC), the NSERC Discovery Grant (RGPIN-2020-05573) to Kheyrollah Pour, Canada Excellent Research Chair-Global Water Futures (CERC-GWF) Remotely Sensed Monitoring of Northern Lake Ice project (grant no. 353374), and the Government of Northwest Territories, Environment Climate Change, the Cumulative Impact Monitoring Programme (project no. CIMP-212). This research was enabled in part by support provided by Compute Ontario (https://www.computeontario.ca/, last access: 28 April 2023) and the Digital Research Alliance of Canada (https://alliancecan.ca/en, last access: 28 April 2023).

References

Adamowski, J., Prokoph, A., 2013. Assessing the impacts of the urban heat island effect on streamflow patterns in Ottawa, Canada. J. Hydrol. 496, 225–237. https://doi.org/10.1016/j.jhydrol.2013.05.032.

Attiah, G., Kheyrollah Pour, H., Scott, K.A., 2023. Lake surface temperature retrieved from Landsat satellite series (1984 to 2021) for the North Slave Region. Earth Syst. Sci. Data 15, 1329–1355. https://doi.org/10.5194/essd-15-1329-2023.

, 2022Attiah, G., Kheyrollah Pour, H., Scott, K.A., 2022. NorthSlave Lake Surface Temperature Retrieved from Landsat Archives from 1984 to 2021. https://doi.org/10.5683/SP3/J4GMC2.

Austin, J.A., Colman, S.M., 2007. Lake Superior summer water temperatures are increasing more rapidly than regional temperatures: a positive ice-albedo feedback. Geophys. Res. Lett. 34, 1–5. https://doi.org/10.1029/2006GL029021.

Avdan, U., Jovanovska, G., 2016. Algorithm for automated mapping of land surface temperature using LANDSAT 8 satellite data. J. Sens. 2016 https://doi.org/10.1155/2016/1480307.

Bachmann, R.W., Sharma, S., Jr, D.E.C., Lecours, V., 2019. The distribution and prediction of summer near-surface water temperatures in lakes of the coterminous United States and Southern Canada. Geosci. 18–20.

Bengtsson, L., 2012. Ice Covered Lakes BT - Encyclopedia of Lakes and Reservoirs. https://doi.org/10.1007/978-1-4020-4410-6.

Cai, Y., Ke, C.Q., Li, X., Zhang, G., Duan, Z., Lee, H., 2019. Variations of lake ice phenology on the tibetan plateau from 2001 to 2017 based on MODIS data. J. Geophys. Res. Atmos. 124, 825–843. https://doi.org/10.1029/2018JD028993.

Carpino, O.A., Berg, A.A., Quinton, W.L., Adams, J.R., 2018. Climate change and permafrost thaw-induced boreal forest loss in northwestern Canada. Environ. Res. Lett. 13 https://doi.org/10.1088/1748-9326/aad74e.

Carrea, L., Merchant, C.J., 2019. GloboLakes: lake surface water temperature (LSWT) v4.0 (1995-2016). Cent. Environ. Data Anal. https://doi.org/10.5285/76a29c5b55204b66a40308fc2ba9cdb3.
Crosman, E.T., Horel, J.D., 2009. Remote sensing of environment MODIS-derived surface temperature of the great salt lake. Remote Sens. Environ. 113, 73–81. https://doi.org/10.1016/j.rse.2008.08.013.
Daufresne, M., Lengfellner, K., Sommer, U., 2009. Global warming benefits the small in aquatic ecosystems. Proc. Natl. Acad. Sci. U. S. A. 106, 12788–12793. https://doi.org/10.1073/pnas.0902080106.
Dauginis, A., Brown, L., 2021. Recent changes in Pan-Arctic sea ice, lake ice, and snow on/off timing. Cryosph. Discuss. 1–35. https://doi.org/10.5194/tc-2021-52.
De Stasio, B.T., Golemgeski, T., Livingstone, D.M., 2014. Temperature as a Driving Factor in Aquatic Ecosystems☆. In: Reference Module in Earth Systems and Environmental Sciences. Elsevier. https://doi.org/10.1016/B978-0-12-409548-9.09051-5.
Dibike, Y., Prowse, T., Saloranta, T., Ahmed, R., 2011. Response of Northern Hemisphere lake-ice cover and lake-water thermal structure patterns to a changing climate. Hydrol. Process. 25, 2942–2953. https://doi.org/10.1002/hyp.8068.
Dokulil, M.T., de Eyto, E., Maberly, S.C., May, L., Weyhenmeyer, G.A., Woolway, R.I., 2021. Increasing maximum lake surface temperature under climate change. Clim. Change 165, 1–18. https://doi.org/10.1007/s10584-021-03085-1.
Eastman, R., Warren, S.G., 2013. A 39-yr survey of cloud changes from land stations worldwide 1971-2009: Long-term trends, relation to aerosols, and expansion of the tropical belt. J. Clim. 26, 1286–1303. https://doi.org/10.1175/JCLI-D-12-00280.1.
Echeverría, S., Hausner, M.B., Bambach, N., Vicuña, S., Suárez, F., 2019. Modeling present and future ice covers in two Antarctic lakes. J. Glaciol. 66, 11–24. https://doi.org/10.1017/jog.2019.78.
Eichler, T.P., Gaggini, N., Pan, Z., 2013. Impacts of global warming on Northern Hemisphere winter storm tracks in the CMIP5 model suite. J. Geophys. Res. Atmos. https://doi.org/10.1002/jgrd.50286.
Flato, G.M., Brown, R.D., 1997. Variability and climate sensitivity of landfast Arctic sea ice. Oceanogr. Lit. Rev. 44, 548.
Guo, L., Zheng, H., Wu, Y., Fan, L., Wen, M., Li, J., Zhang, F., Zhu, L., Zhang, B., 2022. An integrated dataset of daily lake surface water temperature over Tibetan Plateau. Earth Syst. Sci. Data Discuss. 1–15.
Hillmer, I., van Reenen, P., Imberger, J., Zohary, T., 2008. Phytoplankton patchiness and their role in the modelled productivity of a large, seasonally stratified lake. Ecol. Modell. 218, 49–59. https://doi.org/10.1016/j.ecolmodel.2008.06.017.
Hook, S.J., Chander, G., Barsi, J.A., Alley, R.E., Abtahi, A., Palluconi, F.D., Markham, B.L., Richards, R.C., Schladow, S.G., Helder, D.L., 2004. In-flight validation and recovery of water surface temperature with Landsat-5 thermal infrared data using an automated high-altitude lake validation site at Lake Tahoe. IEEE Trans. Geosci. Remote Sens. 42, 2767–2776. https://doi.org/10.1109/TGRS.2004.839092.
Huang, Y., Liu, H., Hinkel, K., Yu, B., Beck, R., Wu, J., 2017. Analysis of thermal structure of arctic lakes at local and regional scales using in situ and multidate landsat-8 data. Water Resour. Res. 53, 9642–9658. https://doi.org/10.1002/2017WR021335.
Jiménez-Munoz, J.C., Sobrino, J.A., 2003. A generalised single-channel method for retrieving land surface temperature from remote sensing data. J. Geophys. Res. Atmos. 108 https://doi.org/10.1029/2003jd003480.
Kendall, M.G., 1975. Rank Correlation Methods, fourth ed. Charles Griffin, London.
Kheyrollah Pour, H., Duguay, C.R., Martynov, A., Brown, L.C., 2012. Simulation of surface temperature and ice cover of large northern lakes with 1-D models: a comparison with MODIS satellite data and in situ measurements. Tellus, Ser. A Dyn. Meteorol. Oceanogr. 64 https://doi.org/10.3402/tellusa.v64i0.17614.
Kheyrollah Pour, H., Duguay, C.R., Scott, K.A., Kang, K.K., 2017. Improvement of lake ice thickness retrieval from MODIS satellite data using a thermodynamic model. IEEE Trans. Geosci. Remote Sens. 55, 5956–5965. https://doi.org/10.1109/TGRS.2017.2718533.
Kuchar, L., Broszkiewicz-Suwaj, E., Iwanski, S., Jelonek, L., 2019. Comparison of daily flows simulated for the year 2060 on the Kaczawa River for various scenarios of climate change by simple time series analysis. E3S Web Conf. 100 https://doi.org/10.1051/e3sconf/201910000041.
Laing, J., Binyamin, J., 2013. Climate change effect on winter temperature and precipitation of Yellowknife, Northwest Territories, Canada from 1943 to 2011. Am. J. Clim. Chang. 02, 275–283. https://doi.org/10.4236/ajcc.2013.24027.
Lang, J., Ma, Y., Li, Z., Su, D., 2021. The impact of climate warming on lake surface heat exchange and ice phenology of different types of lakes on the tibetan plateau. Water (Switz.) 13. https://doi.org/10.3390/w13050634.
Leppäranta, M., Wang, K., 2008. The ice cover on small and large lakes: Scaling analysis and mathematical modelling. Hydrobiologia 599, 183–189. https://doi.org/10.1007/s10750-007-9201-3.
Lieberherr, G., Wunderle, S., 2018. Lake surface water temperature derived from 35 years of AVHRR sensor data for European lakes. Remote Sens 10. https://doi.org/10.3390/rs10070990.
Livingstone, D.M., 2003. Impact of secular climate change on the thermal structure of a large temperate Central European lake. Clim. Change 57, 205–225. https://doi.org/10.1023/A:1022119503144.
Livingstone, D.M., Lotter, F., Kettle, H., 2005. Altitude-dependent differences in the primary physical response of mountain lakes to climatic forcing. Limnol. Oceanogr. 50, 1313–1325.
Long, Z., Perrie, W., Gyakum, J., Caya, D., Laprise, R., 2007. Northern lake impacts on local seasonal climate. J. Hydrometeorol. 8, 881–896. https://doi.org/10.1175/JHM591.1.
Magee, M.R., Wu, C.H., 2017. Response of water temperatures and stratification to changing climate in three lakes with different morphometry. Hydrol. Earth Syst. Sci. 21, 6253–6274. https://doi.org/10.5194/hess-21-6253-2017.
Mason, L.A., Riseng, C.M., Gronewold, A.D., Rutherford, E.S., Wang, J., Clites, A., Smith, S.D.P., McIntyre, P.B., 2016. Fine-scale spatial variation in ice cover and surface temperature trends across the surface of the Laurentian Great Lakes. Clim. Change 138, 71–83. https://doi.org/10.1007/s10584-016-1721-2.
Matzinger, A., Schmid, M., Veljanoska-Sarafiloska, E., Patceva, S., Guseska, D., Wagner, B., Müller, B., Sturm, M., Wüest, A., 2007. Eutrophication of ancient Lake Ohrid: Global warming amplifies detrimental effects of increased nutrient inputs. Limnol. Oceanogr. 52, 338–353. https://doi.org/10.4319/LO.2007.52.1.0338.
Ménard, P., Duguay, C.R., Flato, G.M., Rouse, W.R., 2002. Simulation of ice phenology on Great Slave Lake, Northwest Territories, Canada. Hydrol. Process. 16, 3691–3706. https://doi.org/10.1002/hyp.1230.
Messager, M.L., Lehner, B., Grill, G., Nedeva, I., Schmitt, O., 2016. Estimating the volume and age of water stored in global lakes using a geo-statistical approach. Nat. Commun. 7 (1), 11. https://doi.org/10.1038/ncomms13603.
Moss, B., 2012. Cogs in the endless machine: Lakes, climate change and nutrient cycles: a review. Sci. Total Environ. 434, 130–142. https://doi.org/10.1016/j.scitotenv.2011.07.069.
Mullan, D., Swindles, G., Patterson, T., Galloway, J., Macumber, A., Falck, H., Crossley, L., Chen, J., Pisaric, M., 2017. Climate change and the long-term viability of the World's busiest heavy haul ice road. Theor. Appl. Climatol. 129, 1089–1108. https://doi.org/10.1007/s00704-016-1830-x.
Niedrist, G.H., Psenner, R., Sommaruga, R., 2018. Climate warming increases vertical and seasonal water temperature differences and inter-annual variability in a mountain lake. Clim. Change 151, 473–490. https://doi.org/10.1007/s10584-018-2328-6.
NOAA. Annual 2021 Global Climate Report. National Ocean Service website, https://www.ncei.noaa.gov/access/monitoring/monthly-report/global/202113, accessed on 7/8/22.
North, R.P., North, R.L., Livingstone, D.M., Köster, O., Kipfer, R., 2014. Long-term changes in hypoxia and soluble reactive phosphorus in the hypolimnion of a large temperate lake: consequences of a climate regime shift. Glob. Chang. Biol. 20, 811–823. https://doi.org/10.1111/GCB.12371.
Ogilvie, A., Belaud, G., Massuel, S., Mulligan, M., Le Goulven, P., Malaterre, P.O., Calvez, R., 2018. Combining Landsat observations with hydrological modelling for improved surface water monitoring of small lakes. J. Hydrol. 566, 109–121. https://doi.org/10.1016/j.jhydrol.2018.08.076.
O'Reilly, C.M., Rowley, R.J., Schneider, P., Lenters, J.D., Mcintyre, P.B., Kraemer, B.M., 2015. Rapid and highly variable warming of lake surface waters around the globe. Geophysical Research Letters, 42: 1-9. Geophys. Res. Lett. 1–9. https://doi.org/10.1002/2015GL066235.Received.
Persaud, B.D., Chasmer, L.E., Quinton, W.L., Wolfe, B.B., English, M.C., 2022. Sensitivity of seasonal air temperature and precipitation, and onset of snowmelt, to Arctic Dipole modes across the Taiga Plains, Northwest Territories, Canada. Int. J. Climatol. 1–18. https://doi.org/10.1002/joc.7810.

Peterson, S.M., Streby, H.M., Andersen, D.E., 2016. Spatially explicit models of full-season productivity and implications for landscape management of Golden-winged Warblers in the western Great Lakes Region. In: Golden-Winged Warbler Ecology, Conservation, and Habitat Management (Studies in Avian Biology, Volume 49). CRC Press, Boca Raton, FL, pp. 141–160.
Petrone, R.M., Rouse, W.R., Marsh, P., 2000. Synoptic controls on the surface energy and water budgets in sub-arctic regions of Canada. Int. J. Climatol. 20, 1149–1165. https://doi.org/10.1002/1097-0088(200008)20:10<1149::AID-JOC527>3.0.CO;2-M.
Pokhrel, Y., Felfelani, F., Satoh, Y., Boulange, J., Burek, P., Gädeke, A., Gerten, D., Gosling, S.N., Grillakis, M., Gudmundsson, L., Hanasaki, N., Kim, H., Koutroulis, A., Liu, J., Papadimitriou, L., Schewe, J., Müller Schmied, H., Stacke, T., Telteu, C.E., Thiery, W., Veldkamp, T., Zhao, F., Wada, Y., 2021. Global terrestrial water storage and drought severity under climate change. Nat. Clim. Chang. 11, 226–233. https://doi.org/10.1038/s41558-020-00972-w.
Pouw, A.F., Kheyrollah Pour, H., MacLean, A., 2023. Mapping snow depth on Canadian sub-arctic lakes using ground-penetrating radar. Cryosph 17, 2367–2385. https://doi.org/10.5194/tc-17-2367-2023.
Prats, J., Reynaud, N., Rebière, D., Peroux, T., Tormos, T., Danis, P.-A., 2018. LakeSST: Lake Skin Surface Temperature in French inland water bodies for 1999–2016 from Landsat archives. Earth Syst. Sci. Data 10, 727–743. https://doi.org/10.5194/essd-10-727-2018.
Prowse, T.D., Furgal, C., Chouinard, R., Melling, H., Milburn, D., Smith, S.L., 2009. Implications of climate change for economic development in Northern Canada: Energy, resource, and transportation sectors. Ambio 38, 272–281. https://doi.org/10.1579/0044-7447-38.5.272.
Qin, R., Zhao, Z., Xu, J., Ye, J.S., Li, F.M., Zhang, F., 2022. HRLT: a high-resolution (1 d, 1 km) and long-term (1961-2019) gridded dataset for surface temperature and precipitation across China. Earth Syst. Sci. Data 14, 4793–4810. https://doi.org/10.5194/essd-14-4793-2022.
Rafat, A., Kheyrollah Pour, H., Spence, C., Palmer, M.J., MacLean, A., 2023. An analysis of ice growth and temperature dynamics in two Canadian subarctic lakes. Cold Reg. Sci. Technol. 210, 103808 https://doi.org/10.1016/j.coldregions.2023.103808.
Ramón, C.L., Ulloa, H.N., Doda, T., Winters, K.B., Bouffard, D., 2020. Latitude and bathymetry modify lake warming under ice 1–21.
Reinart, A., Reinhold, M., 2008. Mapping surface temperature in large lakes with MODIS data. Remote Sens. Environ. 112, 603–611. https://doi.org/10.1016/j.rse.2007.05.015.
Rouse, W.R., Oswald, C.J., Binyamin, J., Spence, C., Schertzer, W.M., Blanken, P.D., Bussières, N., Duguay, C.R., 2005. The role of northern lakes in a regional energy balance. J. Hydrometeorol. 6, 291–305. https://doi.org/10.1175/JHM421.1.
Rouse, W.R., Binyamin, J., Blanken, P.D., Bussières, N., Duguay, C.R., Oswald, C.J., Schertzer, W.M., Spence, C., 2008. The influence of lakes on the regional energy and water balance of the central Mackenzie River Basin. Cold Reg. Atmos. Hydrol. Stud. Mackenzie GEWEX Exp. Vol. 1 Atmos. Dyn. 309–325. https://doi.org/10.1007/978-3-540-73936-4_18.
Schmid, M., Köster, O., 2016. Excess warming of a Central European lake driven by solar brightening. Water Resour. Res. 52, 8103–8116. https://doi.org/10.1002/2016WR018651.
Schneider, P., Hook, S.J., 2010. Space observations of inland water bodies show rapid surface warming since 1985. Geophys. Res. Lett. 37, 1–5. https://doi.org/10.1029/2010GL045059.
Sen, P.K., 1968. Estimates of the regression coefficient based on Kendall's Tau. J. Am. Stat. Assoc. 63, 1379–1389. https://doi.org/10.1080/01621459.1968.10480934.
Sharma, S., Blagrave, K., Magnuson, J.J., O'Reilly, C.M., Oliver, S., Batt, R.D., Magee, M.R., Straile, D., Weyhenmeyer, G.A., Winslow, L., Woolway, R.I., 2019. Widespread loss of lake ice around the Northern Hemisphere in a warming world. Nat. Clim. Chang. 9, 227–231. https://doi.org/10.1038/s41558-018-0393-5.
Shinohara, R., Tanaka, Y., Kanno, A., Matsushige, K., 2021. Relative impacts of increases of solar radiation and air temperature on the temperature of surface water in a shallow, eutrophic lake. Hydrol. Res. 52, 916–926. https://doi.org/10.2166/nh.2021.148.
Sima, S., Ahmadalipour, A., Tajrishy, M., 2013. Mapping surface temperature in a hyper-saline lake and investigating the effect of temperature distribution on the lake evaporation. Remote Sens. Environ. 136, 374–385. https://doi.org/10.1016/j.rse.2013.05.014.
Sivarajah, B., Cheney, C.L., Perrett, M., Kimpe, L.E., Blais, J.M., Smol, J.P., 2020. Regional gold mining activities and recent climate warming alter diatom assemblages in deep sub-Arctic lakes. Polar Biol. 43, 305–317. https://doi.org/10.1007/s00300-020-02635-0.
Slater, J.A., Garvey, G., Johnston, C., Haase, J., Heady, B., Kroenung, G., Little, J., 2006. The SRTM data "finishing" process and products. Photogramm. Eng. Remote Sens. 72, 237–247. https://doi.org/10.14358/PERS.72.3.237.
Sobrino, J.A., Jiménez-Muñoz, J.C., Paolini, L., 2004. Land surface temperature retrieval from LANDSAT TM 5. Remote Sens. Environ. 90, 434–440. https://doi.org/10.1016/j.rse.2004.02.003.
Song, F., Zhang, G.J., Ramanathan, V., Leung, L.R., 2022. Trends in surface equivalent potential temperature: a more comprehensive metric for global warming and weather extremes. Proc. Natl. Acad. Sci. U. S. A. 119, 1–7. https://doi.org/10.1073/pnas.2117832119.
Song, K., Wang, Min, Du, J., Yuan, Y., Ma, J., Wang, Ming, Mu, G., 2016. Spatiotemporal variations of lake surface temperature across the Tibetan Plateau using MODIS LST product. Remote Sens 8. https://doi.org/10.3390/rs8100854.
Stefanidis, K., Varlas, G., Papaioannou, G., Papadopoulos, A., Dimitriou, E., 2022. Trends of lake temperature, mixing depth and ice cover thickness of European lakes during the last four decades. Sci. Total Environ. 830, 154709 https://doi.org/10.1016/j.scitotenv.2022.154709.
Tom, M., Wu, T., Baltsavias, E., Schindler, K., 2022. Recent ice trends in Swiss Mountain Lakes: 20-year analysis of Modis imagery. PFG - J. Photogramm. Remote Sens. Geoinf. Sci. 90, 413–431. https://doi.org/10.1007/s41064-022-00215-x.
Tye, S.P., Siepielski, A.M., Bray, A., Rypel, A.L., Phelps, N.B., Fey, S.B., 2022. Climate warming amplifies the frequency of fish mass mortality events across north temperate lakes. Limnology and Oceanography Letters 7 (6), 510–519.
Van Cleave, K., Lenters, J.D., Wang, J., Verhamme, E.M., 2014. A regime Shift In Lake Superior Ice Cover, Evaporation, And water temperature following the warm el niño winter of 1997–1998. Limnol. Oceanogr. 59, 1889–1898. https://doi.org/10.4319/lo.2014.59.6.1889.
Vanhellemont, Q., 2020. Automated water surface temperature retrieval from Landsat 8/TIRS. Remote Sens. Environ. 237, 111518 https://doi.org/10.1016/j.rse.2019.111518.
Woolway, R.I., Verburg, P., Merchant, C.J., Lenters, J.D., Hamilton, D.P., Brookes, J., Kelly, S., Hook, S., Laas, A., Pierson, D., Rimmer, A., Rusak, J.A., Jones, I.D., 2017. Latitude and lake size are important predictors of over-lake atmospheric stability. Geophys. Res. Lett. 44, 8875–8883. https://doi.org/10.1002/2017GL073941.
Woolway, R.I., Kraemer, B.M., Lenters, J.D., Merchant, C.J., O'Reilly, C.M., Sharma, S., 2020. Global lake responses to climate change. Nat. Rev. Earth Environ. 1, 388–403. https://doi.org/10.1038/s43017-020-0067-5.
Xie, C., Zhang, X., Zhuang, L., Zhu, R., Guo, J., 2022. Analysis of surface temperature variation of lakes in China using MODIS land surface temperature data. Sci. Rep. https://doi.org/10.1038/s41598-022-06363-9.
Yang, K., Yu, Z., Luo, Y., 2020. Analysis on driving factors of lake surface water temperature for major lakes in Yunnan-Guizhou Plateau. Water Res 184, 116018. https://doi.org/10.1016/j.watres.2020.116018.
Yang, Y., Leppäranta, M., Cheng, B., Li, Z., 2012. Numerical modelling of snow and ice thicknesses in Lake Vanajavesi. Finl. Tellus, Ser. A Dyn. Meteorol. Oceanogr. 64 https://doi.org/10.3402/tellusa.v64i0.17202.
Ye, X., Anderson, E.J., Chu, P.Y., Huang, C., Xue, P., 2019. Impact Of Water Mixing And Ice Formation On The Warming of Lake Superior: A Model-guided Mechanism Study. Limnol. Oceanogr. 64, 558–574. https://doi.org/10.1002/lno.11059.
Yu, S.J., Ryu, I.G., Park, M.J., Im, J.K., 2021. Long-term relationship between air and water temperatures in Lake Paldang, South Korea, 0–3 Environ. Eng. Res. 26. https://doi.org/10.4491/eer.2020.177.
Zhang, G., Yao, T., Chen, W., Zheng, G., Shum, C.K., Yang, K., Piao, S., Sheng, Y., Yi, S., Li, J., O'Reilly, C.M., Qi, S., Shen, S.S.P., Zhang, H., Jia, Y., 2019. Regional differences of lake evolution across China during 1960s–2015 and its natural and anthropogenic causes. Remote Sens. Environ. 221, 386–404. https://doi.org/10.1016/j.rse.2018.11.038.
Zhong, Y., Notaro, M., Vavrus, S.J., Foster, M.J., 2016. Recent accelerated warming of the Laurentian Great LakeS: Physical drivers. Limnol. Oceanogr. 61, 1762–1786. https://doi.org/10.1002/lno.10331.